Perspective

Israel Journal of Chemistry
www.ijc.wiley-vch.de

doi.org/10.1002/ijch.202400061

A Personal Journey in Nanoscience via Developing and Applying Liquid Phase TEM

Haimei Zheng*[a, b]

Abstract: Liquid phase TEM has attracted widespread attention in recent years as a groundbreaking tool to address various fundamental problems in nanoscience. It has provided the opportunity to reveal many unseen dynamic phenomena of nanoscale materials in solution processes by direct imaging through liquids with high spatial and temporal resolution. After my earlier work on real-time imaging of the nucleation, growth, and dynamic motion of nanoparticles in liquids by developing high-resolution liquid phase transmission electron microscopy (TEM) down to the sub-nanometer level, I established my own research group at Lawrence Berkeley National Lab in 2010. My group focuses on developing and applying liquid phase TEM to investigate complex systems and reactions. We have studied a set of scientific problems centered on understanding how atomic level heterogeneity and fluctuations at solid-liquid interfaces impact nanoscale materials transformations using advanced liquid phase TEM. This article describes my personal journey in nanoscience, highlighting the main discoveries of my research group using liquid phase TEM as a unique tool. Some perspectives on the impacts of liquid phase TEM and the future opportunities in nanoscience and nanotechnology enabled by liquid phase TEM are also included.

Keywords: Liquid phase TEM · liquid cell · nanocrystal dynamics · solid-liquid interfaces · nucleation and growth · electrified solid-liquid interfaces

My earlier research focused on oxide thin films. By innovating the transmission electron microscopy (TEM) thin film sample preparation technique (with Prof. Salamanca-Riba) during my Ph.D. study, I was able to achieve high-resolution TEM imaging of thin films directly after hand polishing without the need for ion milling, which drastically improved the speed of sample preparation. It allowed me to prepare and characterize a large number (350–400) of thin oxide film TEM samples, which greatly facilitated the research within then the Materials Research Science and Engineering Center (MRSEC) at University of Maryland, College Park. In parallel, I did thin film growth that led to the publication entitled "multiferroic $BaTiO_3$-$CoFe_2O_4$ nanostructures" in *Science*[1] (with Prof. Ramesh and others). These early research and training profoundly impacted my next research development.

In 2004, I moved to University of California (UC), Berkeley as a senior Ph.D. student with then my advisor, Prof. Ramesh. My research at Berkeley was to study the growth mechanisms of oxide thin film nanostructures using the advanced electron microscopy facility of National Center for Electron Microscopy (NCEM) at Lawrence Berkeley National Lab (LBNL). In the spring of 2006, I completed my research on oxide thin films[1–4] including productive collaboration[2,3] with Dr. Ulrich (Uli) Dahmen, who was the NCEM director at that time. Uli asked me to propose a research project outside of oxide thin films and can take advantage of the Berkeley outstanding scientific environment. He gently suggested developing high-resolution TEM capability for imaging of solid-liquid interfaces of melting liquid alloys. There was a hot paper in *Science* on imaging of the melting liquid metal interfaces at high temperature using high-resolution TEM.[5] But, I only captured part of the suggestion on "developing high-resolution TEM to image some liquid samples". It sounded exotic since all the TEM experiments I knew were imaging of solid samples.

I enthusiastically started to explore the research possibilities by developing high-resolution TEM for imaging of liquid samples. In 1944 a liquid cell was developed with nitrocellulose film on a platinum frame that enabled encapsulation of liquids inside the cell.[6] Such cell design facilitated the later development of micro-sized reactors for *in situ* TEM study of chemical/physical processes in liquid or oil environments. In 1967, Blech *et al.* customized the TEM sample holder tip

[a] Materials Sciences Division, Lawrence Berkeley National Laboratory, Berkeley, CA, USA
[b] Department of Materials Science and Engineering, University of California Berkeley, Berkeley, CA, USA

Correspondence: Haimei Zheng, Materials Sciences Division, Lawrence Berkeley National Laboratory, Berkeley 94720, CA, USA.
Email: hmzheng@lbl.gov

Israel Journal of Chemistry

using a silicon wafer and were able to observe void formation inside aluminum thin films upon electrical stimuli inside TEM.[7] In 2003, Ross' team at IBM developed electrochemical liquid cells using Si with SiN_x viewing window to study electrodeposition of Cu and achieved the spatial resolution of 5 nm.[8] It was very helpful to know that developing Si/SiN_x liquid cells is a viable approach and there was indeed a need to improve the resolution of TEM imaging through liquids. I chatted with many people at Berkeley about my new interest in developing high-resolution TEM for imaging liquid samples. My friend, Prof. Groves in the Department of Chemistry at UC Berkeley, suggested me to apply the new technique to study outstanding research topics. Then, I learned the research on "Physical chemistry of nanocrystals" led by Prof. Alivisatos in the Chemistry Department was among the most prominent at that time in Berkeley. After reading hundreds of papers on nanocrystals, mostly looking for how TEM was used in the research, I gained confidence that developing high-resolution TEM imaging through liquids can be a unique and novel approach to investigate nanocrystals. I proposed to Uli that I would like to "study colloidal nanocrystal growth mechanisms by developing high-resolution TEM imaging through liquids", and I received full support as a postdoc at NCEM. Only later, I realized that imaging of the melting liquid metal under high temperature heating using high-resolution TEM would match Uli′s research interest and it could be fascinating research as well, but a very different research direction.

After the research proposal was approved at NCEM, however, I realized that I had never seen how nanocrystals were synthesized in a real chemistry lab, and I did not have any experience in fabrication of liquid cells or anything in a clean room. I reached out to Prof. Alivisatos and expressed my interest in gaining some experience in nanocrystal synthesis in his lab for my research proposal at NCEM. I got Prof. Alivisatos' enthusiastic support, which was huge encouragement for me. And, I began the liquid cell fabrication through self-training at the Microfabrication Lab at UC Berkeley. Then, my research background on the growth and characterization of oxide thin films helped me tremendously. It still took me almost six months to successfully make the first liquid cell, which was at the end of 2006.

For the early liquid cell TEM experiments at NCEM, I was only allowed to use an old microscope, JEOL3010 with the poorest resolution of ~1 nm at NCEM, due to the management team′s concerns on potential contaminations of liquid samples on the microscopes. In retrospect, not being able to use a high-resolution microscope was perhaps the best arrangement for realizing today′s capability and resolutions of liquid phase TEM, since I single-mindedly focused on designing better and better liquid cells.

In 2010, I became a staff scientist in Materials Sciences Division at LBNL supported by an Laboratory Directed Research and Development (LDRD) project on "Imaging through liquids using a TEM". Subsequently, my research proposal on "Real-time imaging of materials transformation in liquid and gas environment" was funded by DOE Office of Science Early Career Research Program (07/01/2011-07/01/2016). I became the lead-PI of a DOE BES multi-PI research program on "Liquid cell electron microscopy: atomic level heterogeneity and fluctuations at solid-liquid interfaces" (started on 10/01/2016). By developing and applying liquid cell TEM as a unique and powerful platform, it has provided an opportunity for me to explore the wonderful world of nanoscience and nanotechnology. Liquid cell TEM has now been widely accepted with an active international research community. Gordon Research Conference on "Liquid Phase Electron Microscopy" was established in 2020. Researchers from universities, research institutions, and industrial sectors enthusiastically joined the research and discussions. There are a series of commercial products for liquid phase TEM research and development.

In this article, I first briefly introduce my initial research effort on developing high-resolution liquid phase TEM. Then, I will show the efforts of my research group on developing high-resolution liquid phase TEM for handling complex systems and reactions, especially for connecting the reactions in liquid cell nanoreactors with the real-world chemical reactions. We have conducted a series of studies on imaging, understanding, and engineering of nanoscale materials transformations and dynamic solid-liquid interfaces. The materials systems of study include metal, oxides, semiconductors, metal-organic complex, and others. The integrated advanced data analysis and commercialization of liquid cell TEM technology are also discussed. At the end, some perspectives on the future opportunities enabled by liquid phase TEM, and their impacts on nanoscience and nanotechnology are included.

The Early Liquid Cell Development and Breakthroughs

It was a challenging task to make Si/SiN_x liquid cells that can encapsulate a small amount of liquids in a high vacuum environment for TEM imaging, especially for someone without any experience in nanofabrication. With high enthusiasm and hard work, I designed and fabricated the first version of Si/SiN_x liquid cell within the first three months. It included several liquid channels connecting with two liquid reservoirs. However, I found it was impossible to flow liquids into the channels for any of my intended experiments. After troubleshooting by discussing with staff members of the Microfabrication Lab (Dr. Xiaofan Meng and others), I decided to make the simplest sandwich liquid cells (Figure 1a). This simple sandwich cell design was similar to the previously reported design,[8] but thinner liquid cells with improved resolution. A set of modifications were made, for example, 1) using thinner SiN_x membranes, *e.g.*, from the previous 100 nm to 20–25 nm; 2) confining the liquids into a thin liquid film using a "sticky" metal film (In) as the spacer (100 nm or

Israel Journal of Chemistry

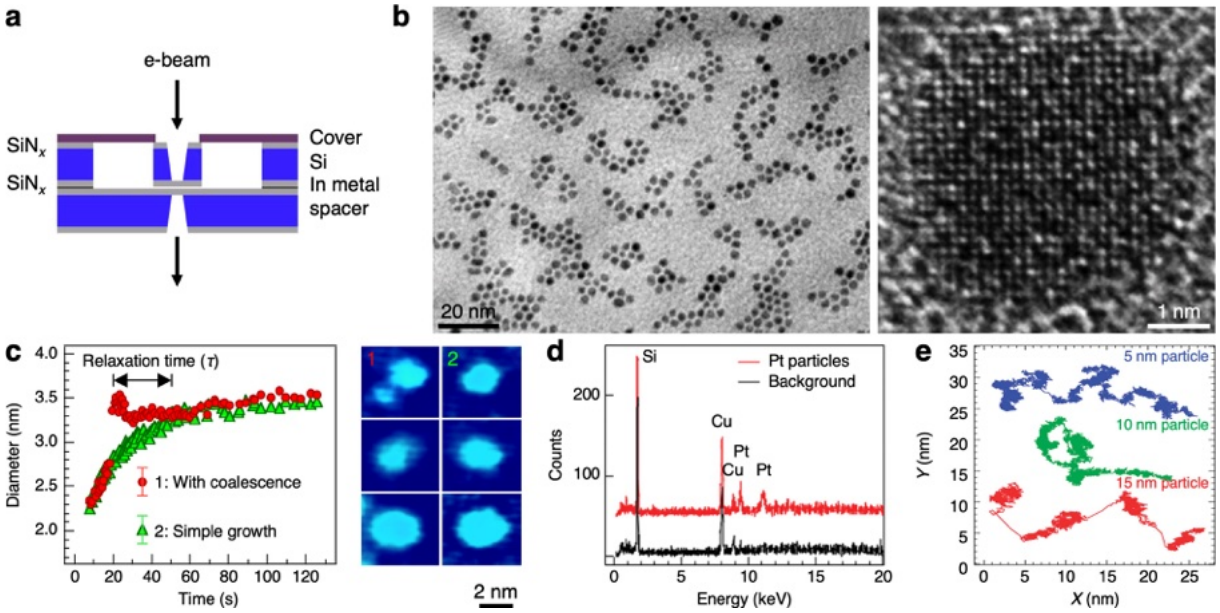

Figure 1. The initial experiments on developing high-resolution liquid cell TEM for imaging and chemical analysis of colloidal nanocrystal nucleation and growth in liquids. (a) A schematic diagram of a liquid cell. (b) TEM image of Pt nanocrystals synthesized inside a liquid cell (left) and high-resolution TEM image of a synthesized Pt nanoparticle selected from the left image (right). (c) Particle diameter as a function of growth time, illustrating two distinct growth trajectories (types 1 and 2) (left) and the corresponding sequential TEM images of the growing nanocrystals (right). (d) EDS spectra of Pt nanoparticles (red) and background (black) obtained *ex-situ* from the liquid cell. (b-d) Reproduced with permission. Copyright 2009, The American Association for the Advancement of Science.[9] (e) Trajectories of 5, 10, and 15 nm sized nanoparticles movements in a liquid film. Reproduced with permission. Copyright 2009, American Chemical Society.[10]

thinner), instead of the previous approach by gluing two chips together; 3) using thinner silicon wafers, *e.g.*, 100 μm instead of the standard 500 μm.

The approach by developing thinner liquid cells was a great success, which enabled breakthroughs in high-resolution imaging through liquids down to the sub-nanometer level. It allowed direct observation of single Pt nanocrystal growth trajectories. As shown in Figure 1b–c, the growth of monodisperse nanoparticles by nanoparticle coalescence and monomer attachment was revealed. Using the thin liquid cells, chemical analysis using energy dispersive X-ray spectroscopy (EDS) through liquids was also achieved for the first time (Figure 1d).[9] By using those liquid cells, tracking dynamic motion of individual nanoparticles was subsequently accomplished (Figure 1e).[10]

These works were the first implementation of liquid phase TEM to study the growth and dynamic motion of colloidal nanoparticles in liquids *down to the sub-nanometer level*, which attracted great attention. Afterwards, there were many groups developing and applying liquid phase TEM for various research topics. At the same time, there were also many skepticisms about the liquid cell TEM method concerning "the electron beam effects", "possible impacts of liquid confinements", "whether it is useful for studying complex reactions", etc. The early success as well as the concerns were the inspiration for my subsequent research exploration.

Nanoscale Materials Transformations Unveiled Via Liquid Phase TEM

Establishing Liquid Phase TEM for Studying Complex Systems and Reactions

After I started my research group at LBNL, we conducted the first set of experiments aiming to establish liquid cell TEM as a tool for studying complex systems and reactions and to address the aforementioned skepticisms and concerns. The efforts were in three categories. 1). Liquid cell experiments at the elevated temperature (*e.g.*, 180 °C) by thermal heating were conducted (Figure 2a–b). Our direct observation revealed fluctuations and oscillatory dynamics of individual Bismuth nanoparticles coupled with the neighboring nanoparticles during growth[11] (Figure 2b). This was a critical work since it demonstrated that it is possible to use the most common stimulus of thermal heating, instead of electron beam irradiation, to initiate the chemical reactions for nanocrystal synthesis. 2). With the control of solution chemistry, we synthesized nanocrystals with various structure and morphology in liquid cells. These early efforts were to show that the observed chemical reactions in a liquid cell are similar to the real-world chemical reactions. We achieved the growth of Pt_3Fe nanorods with a large aspect ratio up to 40 : 1 by nanoparticle attachment. Tracking the formation of individual and chains of nanoparticles enabled the quantification of

Israel Journal of Chemistry

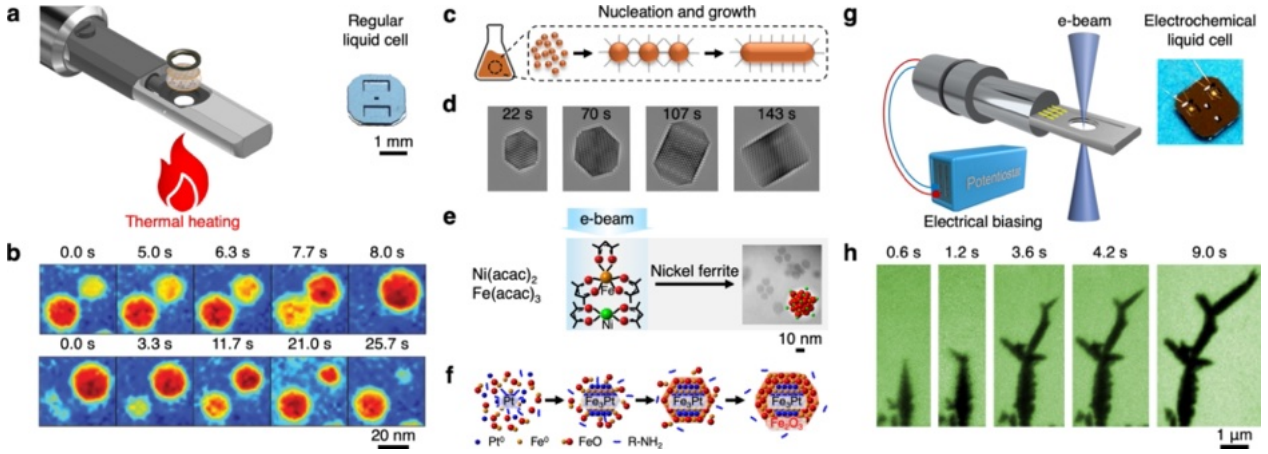

Figure 2. ***In situ*** **liquid cell TEM studies of nanomaterial growth and transformations under various external stimuli**. (a) Conceptual illustration of liquid cell TEM experiments under thermal heating. The picture of thermal heating was reproduced with permission. Copyright 2024, Kru, Adobe Stock, under Education license. (b) Bright-field TEM images with color gradient maps presenting the oscillatory growth of bismuth nanoparticles. Reproduced with permission. Copyright 2012, American Chemical Society.[11] (c) Schematic illustration of the nucleation and growth of one-dimensional nanowires. Reproduced with permission. Copyright 2024, Lidiia Koval, Adobe Stock, under Education license. (d) Sequential HRTEM images showing the growth of Pt nanocube. Reproduced with permission. Copyright 2014, The American Association for the Advancement of Science.[13] (e) Schematic diagram of the growth of nickel ferrite nanocrystals in a liquid cell, along with a representative TEM image of the synthesized nanocrystals. Reproduced with permission. Copyright 2015, American Chemical Society.[15] (f) Diagram of the formation pathway of Fe_3Pt–Fe_2O_3 core–shell nanoparticles in a liquid cell. Reproduced with permission. Copyright 2015, American Chemical Society.[14] (g) Schematic illustration of a TEM biasing holder with a digital photograph of an assembled electrochemical liquid cell in the biasing holder. (h) Time-series TEM images of the growth of Pb dendrites. (g-h) Reproduced with permission. Copyright 2013, The Authors, under a Creative Commons Attribution-NonCommercial-ShareAlike 3.0 Unported License.[16]

interaction forces between nanoparticles and the evolution of atomic crystal structures. This work revealed the liquid cell TEM capability for studying complex liquid phase reactions and nanoparticle self-assembly[12] (Figure 2c). Subsequently, the growth of Pt nanocubes with shape control was also accomplished[13] (Figure 2d). In addition, by systematically varying the precursor solution chemistry, the formation of metal oxide nanocrystals and Pt-catalyzed metal-metal oxide core-shell nanoparticles were also observed[14] (Figure 2e–f). 3). By developing thinner electrochemical liquid cells, we targeted on studying electron beam sensitive systems, such as Li-ion batteries, electrocatalysis, etc. For the initial experiments, dendric growth of Pb at the electrode-electrolyte interfaces was observed[16] (Figure 2g–h). With further improved capability in handling beam/air sensitive materials systems, we also observed lithium dendrite growth/dissolution and solid-electrolyte interphase (SEI) formation.[17,18] The atomic-resolution electrochemical liquid cell study of complex electrocatalytic reactions, e.g., Cu catalysed CO_2 reduction reactions was achieved recently.[29] This set of work contributed to establishing the liquid cell TEM as a powerful tool for studying systems with varied chemistry and complexity under different stimuli, accelerating the applications of liquid phase TEM to researching diverse topics across materials science, chemistry, and beyond.

Liquid Phase TEM with Atomic Resolution and Control of Electron Beam Effects

The ability to image through liquids with high resolution is crucial for resolving the nanoscale materials transformation pathways. With the collective effort of the liquid cell TEM community, a trajectory of fast-improving spatial resolution of liquid cell TEM imaging has been achieved.[19] Figure 3 highlights the improved resolution from the initial low magnification (1940s), to a few nanometers (~5 nm) in 2003,[8] sub-nanometer in 2009,[9,10] atomic resolution in 2012,[12,13,20] and beyond.[22] With thin membrane liquid cells, *e.g.*, graphene,[23] amorphous carbon,[26] MoS_2,[27] BN,[28] polymer membrane,[29] or other two-dimensional (2D) materials and carefully controlled liquid thickness, high-resolution imaging through thin liquids similar to imaging in vacuum (*e.g.*, sub-Armstrong) can be achieved using aberration-corrected TEM. It is important to note that when the liquid cell is made thin enough, the microscope instrument resolution can be readily achieved.

An important issue for applications of liquid cell TEM is to control electron beam effects and distinguish the electron beam-induced chemical reactions from the real-world reactions (Figure 4). The high-energy electron beam interacting with a sample may introduce perturbation to the system of study, and the electron beam effects are categorized as "knock-on" damage, ionization, electron-beam heating, etc.[30] For TEM imaging through liquids, besides the electron beam damage

Israel Journal of Chemistry

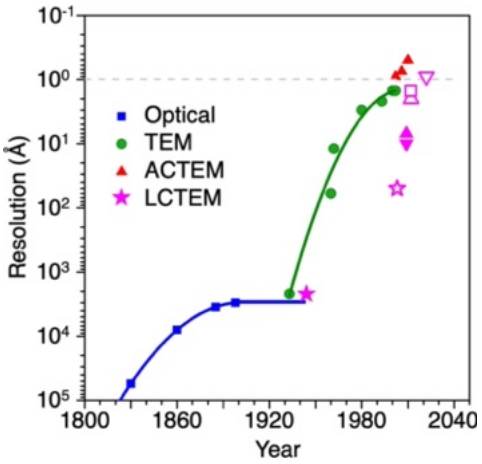

Figure 3. The spatial resolution roadmap of microscopy techniques, including optical microscopy, TEM, aberration-corrected TEM (AC-TEM), and liquid cell TEM (LCTEM). Reproduced with permission. Copyright 2024, The Authors, under a Creative Commons Attribution 4.0 International License.[19]

induced by the primary electrons, secondary electrons and reactive radicals can further react with the sample. These reactions can be dependent on the local environment, such as pH values, composition, diffusion rates/path, gas products, etc. It is a great challenge to quantify the electron beam effects, and it is almost impossible to create one formula that can fit all for the liquid cell TEM experiments.

Effective strategies have been developed to limit the electron beam effects.[19] For example, controlling the electron beam dose can lessen the electron beam damage.[30,31] Thinner liquid cells may reduce electron beam inelastic scattering, thus decreasing the electron beam effects. Additionally, control experiments, such as understanding the electron beam effects by systematically changing the electron beam current density; adding radical scavengers into the solution,[32] *ex situ* control experiments provide valuable reference points for the liquid cell TEM studies. In many cases, knowing how to synthesize nanocrystals in a real chemistry lab is useful to discern some artifacts in the study of nanocrystal growth mechanisms using liquid cell TEM.

Revealing Growth and Transformation Pathways of Colloidal Nanocrystals

The ability to directly observe nanoscale materials growth and transformations at the atomic level opens the opportunities to uncover the underlying mechanisms, contributing to novel materials synthesis and applications. We have studied the formation pathways of various nanoparticles with distinct morphology (beyond quantum dots), for example, nanowires,[12,35] nanocubes,[13] nanosheets,[36] core-shell nanoparticles,[22] and others. Our studies revealed unique growth mechanisms, providing valuable insights into the nature of nanoscale materials. A few selected works are highlighted as follows.

The sequential images in Figure 5a show the formation of a $PtFe_3$ nanowire from a molecular precursor solution, where nanoparticles were formed initially, and they subsequently interacted and attached together to form the nanowire. The atomic structural rearrangements including defect evolution within a nanoparticle were also captured.[12] With advanced image analysis, we were able to further quantify the interaction forces between nanoparticles and their evolution during nano-

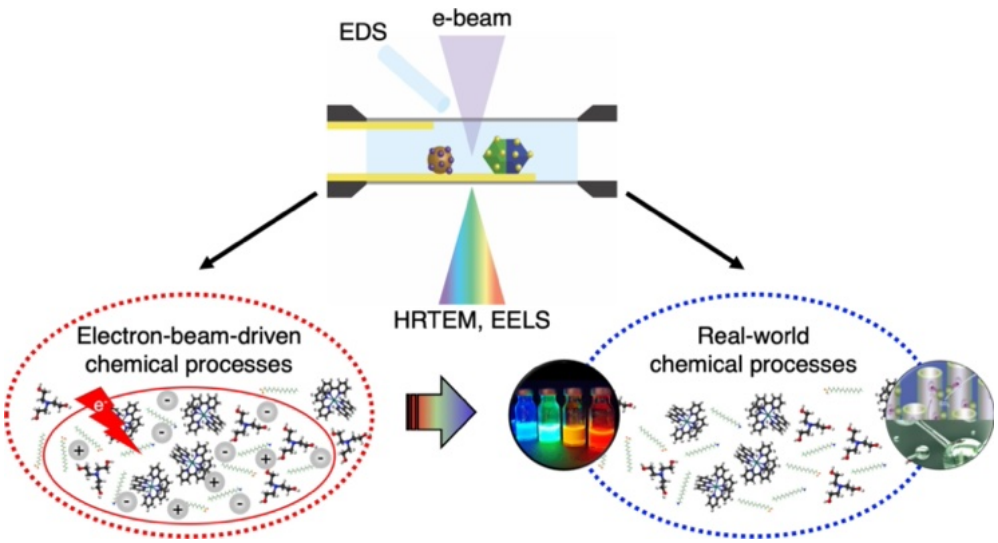

Figure 4. Schematic illustration depicting liquid cell TEM experiments with complementary analysis techniques, linking electron-beam-driven chemical processes to the real-world chemical reactions. Reproduced with permission. Copyright 2024, The Authors, under a Creative Commons Attribution 4.0 International Licenses.[19]

Israel Journal of Chemistry

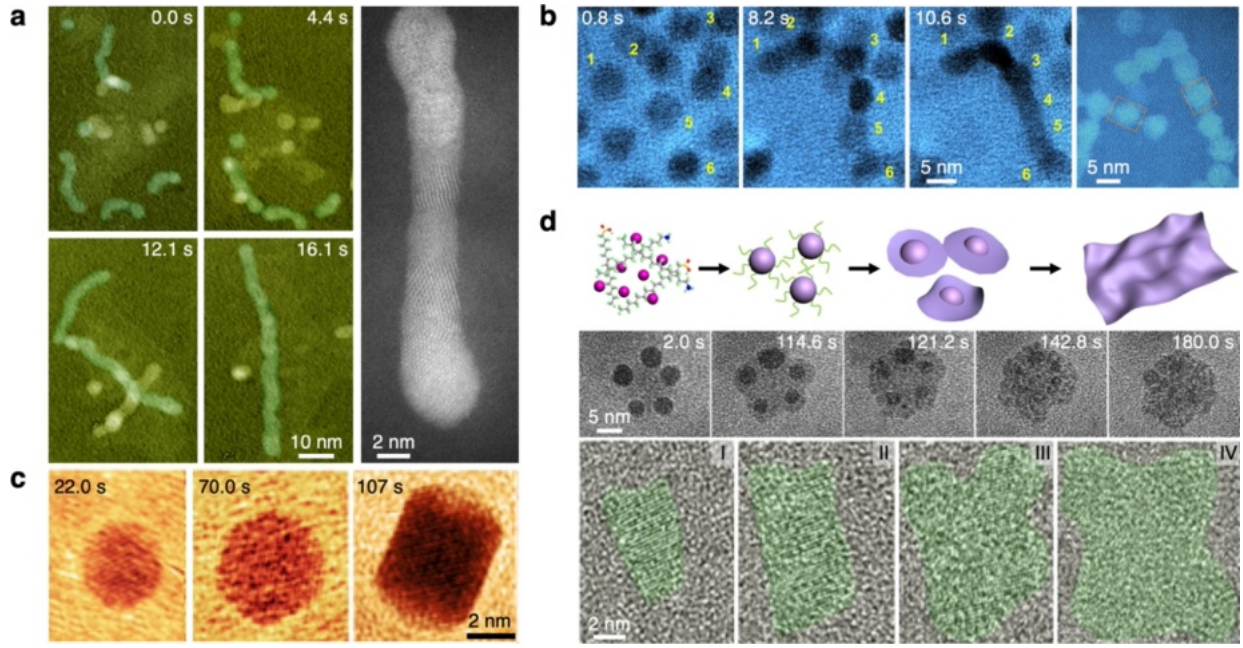

Figure 5. ***In situ*** **liquid cell TEM studies of growth and transformations of nanocrystals with diverse morphorologies, *e.g.*, one-dimensional (1D) nanowires, nanocubes, and 2D nanosheets**. (a) Sequential TEM images illustrating the growth of a Pt_3Fe nanowire through nanoparticle attachments, with high-resolution imaging revealing its polycrystallinity and iron-rich regions. Reproduced with permission. Copyright 2012, The American Association for the Advancement of Science.[12] (b) Time-lapse TEM images showing an initial 2D hexagonal monolayer transforms into a 1D chain *via* oriented attachment of PdSe nanocrystals. Reproduced with permission. Copyright 2019, The Authors, under a Creative Commons Attribution-NonCommercial License 4.0.[35] (c) Time-series simulated HRTEM images demonstrating the growth of a Pt nanocube. Reproduced with permission. Copyright 2014, The American Association for the Advancement of Science.[13] (d) Diagram showing the formation of a 3D oxide nanoparticle and its subsequent transformation into a 2D nanosheet (first row). Time-series TEM images of the 3D-to-2D transformation of cobalt nickel oxide nanoparticles (second row). Sequential HRTEM images of the growth of a 2D cobalt oxide nanosheet (third row). Reproduced with permission. Copyright 2019, This is a U.S. government work and not under copyright protection in the U.S.; foreign copyright protection may apply.[36]

particle self-assembly.[37] Using semiconductor nanocrystal PbSe as a model system,[35] we found individual nanocrystals may experience shape changes due to inter-particle interactions during superlattice transformations. When the oleate ligands were removed from the PbSe nanoparticle surfaces within a honeycomb superlattice by a solution of ethylene glycol (EG) with ethylenediamine (EDA) (EDA:EG = 1 : 1000), an individual nanocrystal displayed dramatic shape changes, up to 40%. Two adjacent nanoparticles formed necking[38] and eventually, a uniform nanowire was achieved before the hexagonal lattice transformed into a square lattice (Figure 5b). The deformation is recoverable when they move apart. Through systematic studies with control experiments and molecular dynamic (MD) simulations, we found that the deformation was due to surface chemistry changes during ligand exchange. The fast ligand removal on the PbSe surfaces may introduce stochiometric changes (Pb : Se ratio) on the nanocrystal surface[39] thus generating electrostatic dipolar interactions between nanocrystals.

Using liquid cell TEM, we tracked the growth of Pt nanocubes[13] (Figure 5c). To rationalize the growth of nanocrystals with distinct facets and shape evolution, both thermodynamic Wulff construction[40] and kinetic factors (*e.g.*, growth rates,[42] surfactants[44]) were considered. Our direct observation revealed that interestingly, the growth of nanocrystals was largely stochastic with no distinct differences in the growth rate until a critical size ($d_c = 2.5$ nm) was reached. About the critical size[13] facets stopped growing and {110} facets continued to grow until an edge was formed, whereas the growth of {111} facets filled the corners of the nanocube. Density functional theory (DFT) calculation revealed that the different mobilities of the ligands on the different facets play an important role. For example, the mobility of ligands is several orders of magnitude lower on the {100} than the {111} facets, thus retarding the growth of the {100} facets. Thus, a selective facet-arrested shape control mechanism, mediated by the ligand mobility on different facets, was proposed.

Our observation of the growth of 2D cobalt oxide or cobalt nickel oxide showed a nanoparticle-mediated growth mechanism, which is different from the previously reported growth by attachment of primary three-dimensional (3D) nanocrystals[46] or the "soft template"-assisted growth of 2D nanostructure.[48] Our direct observation revealed that nanoparticles were formed from a precursor solution initially. When these nanoparticles reached a critical size (*e.g.*, ~4 nm for cobalt oxide), they transformed into 2D nanosheets (Fig-

ure 5d). The 3D-to-2D transformation is unique. Our theoretical calculation suggested a shape factor should be considered for understanding the transformation mechanisms.[36]

Another highlight of our work is on the ripening of core-shell nanostructures with cadmium-cadmium chloride core-shell nanostructures (Cd-$CdCl_2$) as a model system.[22] Sequential images and the corresponding schematic show the structure evolution of core-shell nanoparticles during ripening (Figure 6a–b). Mass transport between particles was mediated by defects and independent of nanoparticle sizes. The core of a nanoparticle (P2) was first dissolved into the solution through the defect sites in the shell, and the growth of another nanoparticle (P1) was achieved by first creating cracks in its shell. The shell structure fluctuated between crystalline and disordered states, leading to the generation and annihilation of crack defects. The defects-mediated ripening is distinctly different from any reported ripening processes, such as Ostwald ripening,[51] digestive ripening,[52] intra-particle ripening,[53] and merging of core-shell particles.[54] Our kinetic Monte Carlo simulation with a simplified lattice model reproduced the basic kinetic processes observed in the liquid phase TEM experiments (see the representative simulated structural evolution in Figure 6c). The fact that the basic kinetic processes were reproduced with a highly simplified model suggests that the mechanism of defects mediated ripening is general and it likely occurs in other core-shell nanoparticles.

In addition, we studied a set of nanocrystal transformations during etching, for example, the effect of ligands on nanocrystal shape evolution during etching,[55] the effect of defects in coating on etching of metal nanoparticles,[56] and other phenomena. The nanocrystal transformations by etching can be viewed as the reverse processes of growth. Thus, imaging and understanding of the dynamic structural evolution during etching are useful for the design and control of nanoscale materials synthesis and discovery.

Remarkable Nanoscale Materials Phenomena

Solid vs. Liquids

Solid and liquid are distinct states of matter in bulk. A solid is described as a substance with fixed atoms that cannot move freely except to vibrate and thus retain its size and shape; while a liquid can flow and keep no definite shape. A range of dynamic phenomena have been considered unique to liquid droplets or nanojets, such as the slip motion of liquid droplets resulting from shape changes,[57] breakdown of liquid nanojets into droplets due to local fluctuations.[60] However, many of our studies implied that such a distinction between solid and liquid is blurred in nanoscale materials during solution processes.

Figure 7a shows that a Pt–Fe nanowire formed in a liquid cell broke down into nanoparticles.[62] The location where the

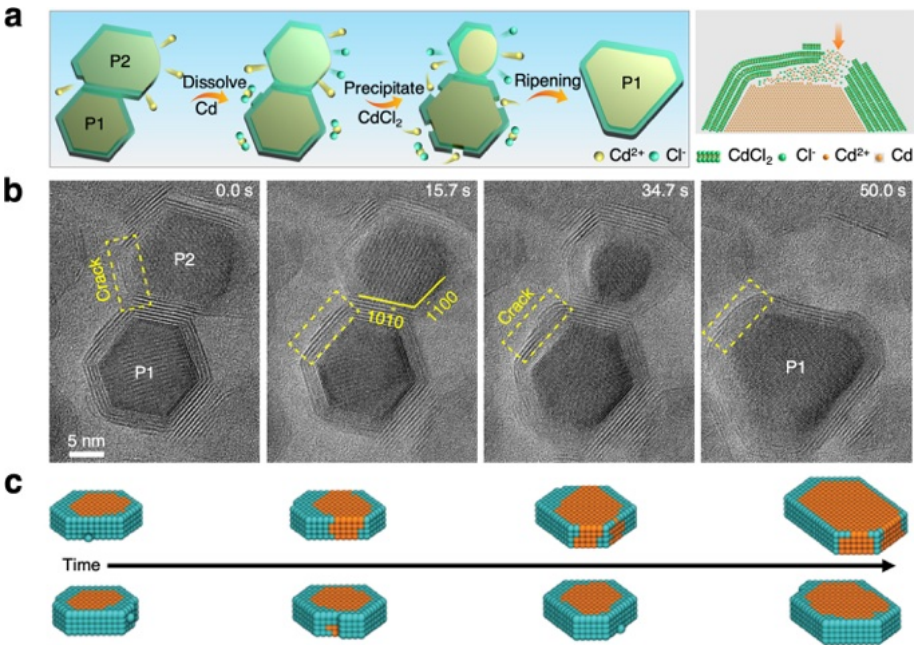

Figure 6. Liquid cell TEM study of defect-mediatedcore-shell nanocrystal transformations. (a) Schematics illustrating the defect-mediated ripening of Cd-$CdCl_2$ core-shell nanocrystals (left) and the influence of defects on Cd core growth during the transformation (right). (b) Time-series HRTEM images of Cd-$CdCl_2$ core-shell nanostructures corresponding to the left schematic in (a). (c) Lattice model depicting the defect-mediated ripening process of core-shell nanostructures. (a-c) Reproduced with permission. Copyright 2022, The Authors, under a Creative Commons Attribution 4.0 International License.[22]

Israel Journal of Chemistry

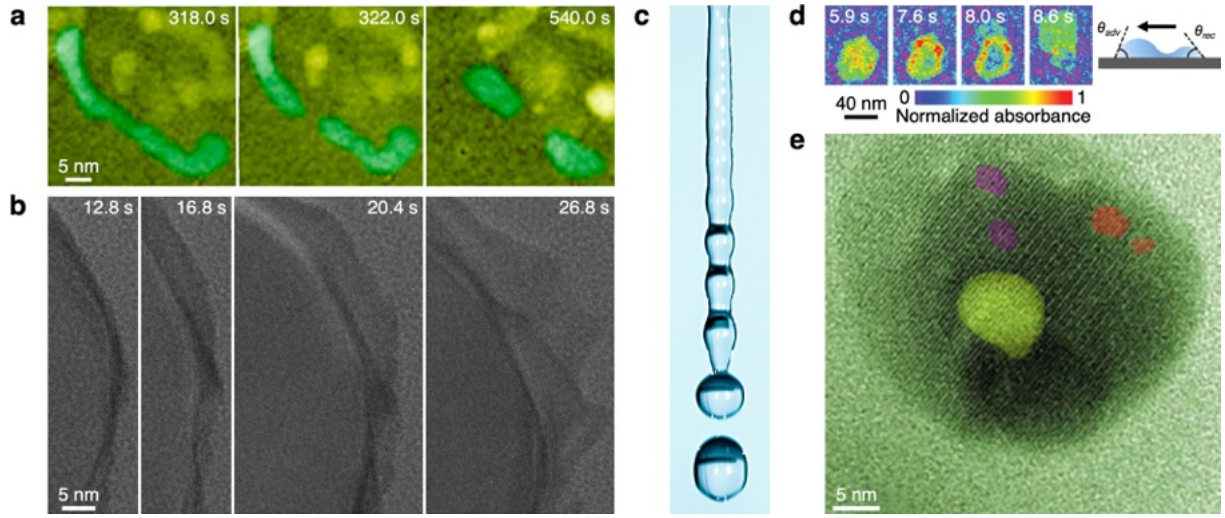

Figure 7. *In situ* investigations of fluid-like behaviors of nanomaterials in liquid cells. (a) Time-series TEM images showing the breakdown and shrinkage of a platinum iron nanowire into nanoparticles. Reproduced with permission. Copyright 2013, American Chemical Society.[62] (b) Consecutive HRTEM images depicting ocean wave-like movements of a Sn nanocrystal during its etching process. Reproduced with permission. Copyright 2024, The Authors, under a Creative Commons Attribution 4.0 International License.[56] (c) Digital photograph visualizing the Plateau–Rayleigh instability. Reproduced with permission. Copyright 2024, SANKOWSKI.IT, Adobe Stock, under Education license. (d) Consecutive TEM intensity maps of a water nanodroplet showing its stick-slip movement, along with a schematic of a cross-sectional view of the droplet with contact angles during the stepping process. Reproduced with permission. Copyright 2012, The Authors.[58] (e) HRTEM image of a Pb-Fe_3O_4 core-shell nanoparticle with gas nanobubbles corresponding to colored regions in the particle. Reproduced with permission. Copyright 2015, The Authors.[74]

breakdown was initiated displayed a thinner diameter, and resulting segments became round to form droplet-like nanoparticles. The observed evolution of the solid nanowire is very similar to the liquid nanojet breakdown into droplets due to Plateau–Rayleigh instability[63] (Figure 7c). Figure 7b shows the evolution of Sn nanoparticles during etching.[56] The interfaces show fascinating shape evolution while maintaining a high crystalline structure. Such curvy morphology evolution is considered, intuitively, to be associated with the behavior of liquids (*e.g.*, Figure 7d). Understanding these dynamic phenomena of solids at the nanoscale, including how external driving forces imposed by thermal, chemical, topographic gradients or surface tension interact with the nanoscale materials, is relevant to broad physical, chemical, and biological processes. Our observations open opportunities to further explore the underlying mechanisms, correlating the nanoscale phenomena with properties and applications of nanoscale materials.

Defects Formation and Healing

Nanoscale materials may experience reversible[65] or irreversible[71] structural transformations during synthesis,[11,65,66] catalytic reactions,[67,68] or other physicochemical processes.[69,70,73] Defects have been found to significantly impact nanoscale materials transformation pathways.[22] As shown in the core-shell nanoparticle ripening (Figure 6), the growth of the core was accomplished by mass diffusion through cracks in the shell, during which the generation and annihilation of cracks were captured. It demonstrated that nanoscale materials are less rigid compared to their bulk counterpart.

Figure 7e shows the generation and migration of oxygen gas bubbles in a nanocrystal when it transforms from iron hydroxide to iron oxide.[74] Geometric phase analysis (GPA) of the crystal lattice revealed an inhomogeneous strain field at a gas bubble. Further computation modeling suggested that the elastic interaction between the core and the bubble provided a driving force for the bubble migration during the dehydration reaction. It is remarkable that any lattice distortion during oxygen gas migration through the lattice can be quickly healed, resulting in a perfect crystal at the end. The nature of nanoscale materials' structural flexibility may be utilized for novel synthesis and engineering of nanoscale materials.

Quasi-Liquid Interphase

A quasi-liquid interphase was found on indium (In) nanocrystal surfaces in an aqueous solution due to oxidative etching.[75] During the etching process, the quasi-liquid phase underwent dynamic configuration changes while maintaining an average thickness of 2–3 nm (Figure 8a). The quasi-liquid phase is different from the traditional understanding of solids or liquids. It contains a high concentration of metal ions and nanoclusters. Direct nucleation and growth of metal clusters from the quasi-liquid phase were observed, which indicates

Israel Journal of Chemistry

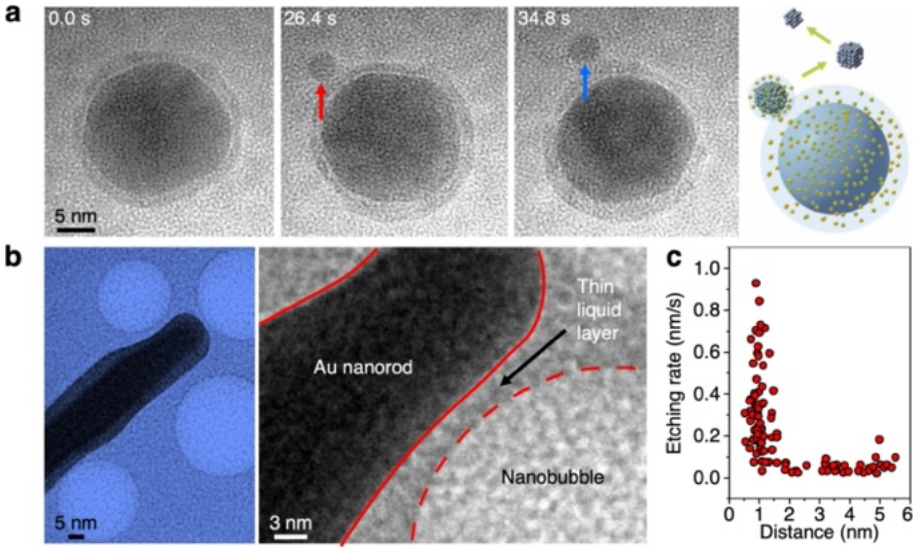

Figure 8. Revealing the roles of solid-liquid interfaces in etching of nanocrystals. (a) Time-series TEM images and corresponding illustration demonstrating a quasi-liquid interphase on the surface of an In nanocrystal, facilitating the dissolution of In nanoclusters (indicated by red and blue arrows). Reproduced with permission. Copyright 2022, The Authors, under a Creative Commons Attribution 4.0 International License.[75] (b) TEM images showing accelerated etching of an Au nanorod near O_2 gas nanobubbles (left) and a magnified view of a thin liquid layer between the nanorod and the nanobubble (right). (c) Etching rate of an Au nanorod as a function of the distance between the nanorod surface and O_2 nanobubble, demonstrating that closer O_2 nanobubbles result in a faster etching rate. (b-c) Reproduced with permission. Copyright 2022, The Authors, under exclusive license to Springer Nature Limited.[78]

that the quasi-liquid interphase acts as a medium for mass transfer between the metal core and the surrounding solution.

A viscous liquid-like phase was also reported when Pb nanocrystals reacted with CH_3O fragments from the triethylene glycol solution under electron beam irradiation.[73] Such a liquid-like phase [$Pb(CH_3O)_2$] can form on the surface of the Pb nanocrystal, or the whole Pb nanocrystal can be converted into [$Pb(CH_3O)_2$]. Swift phase transformations between the liquid-like phase and crystalline Pb solid were captured. This suggests the potential applications of the metal nanoparticles in sensing, drug delivery, or others.

Solid-Liquid-Gas Interfaces

Gaseous reactants often represent at the solid-liquid interfaces and participate in reactions. There have been reports that reaction rates can be notably enhanced by delivering gases directly to the solid surfaces.[76] However, how the gas accelerates the reactions at the triple-phase interface is often unclear due to the lack of quantitative analysis regarding reaction kinetics and the mechanisms of gas transport to the triple-phase interfaces.

We discovered the accelerated etching of gold nanorods by oxygen nanobubbles in an aqueous hydrobromic acid solution by real-time observation using liquid phase TEM.[78] Figure 8b–c shows an order of magnitude enhanced etching rate when oxygen nanobubbles are in close vicinity (~1 nm). Further theoretical simulation indicated that when this distance was reduced below the critical threshold (*e.g.*, 1 nm), O_2 molecules can be readily adsorbed onto the Au nanorod surface due to the strong attractive van der Waals interactions. The participation of O_2 may assist the etching kinetics. However, when the distance between O_2 molecules and the nanorod surface is beyond the critical threshold, O_2 molecules may diffuse slowly showing negligible impact. This work provided critical insights into engineering reactions by controlling solid-liquid interfaces.

Electrified Solid-Liquid Interfaces

Solid-liquid interfaces play an important role in various physical, chemical, and electrochemical processes. Solid-liquid interfaces are intrinsically heterogeneous, for example, there may be charge accumulation, adsorbents, etc., which can significantly impact the properties of nanoscale materials and their applications. For instance, in electrocatalysis or other energy devices,[79] electron and mass transport occur at the electrified solid-liquid interfaces. Structural modifications of the interfaces may drastically influence the electrocatalytic reactions. Direct probing electrified solid-liquid interfaces is challenging, due to the nature of nanoscale geometry, being buried in liquids, the dynamic processes and the complex local environment.

We made high-resolution electrochemical liquid cells, allowing us to directly monitor the dynamic phenomena at electrified solid-liquid interfaces, including deposition/dissolu-

Israel Journal of Chemistry

tion, electrocatalytic structural transformation, and others. Some of our works using electrochemical liquid cell TEM are highlighted as follows.

Dendritic Growth, SEI, Electrolyte Structural Ordering in Batteries

We developed Si/SiN_x electrochemical liquid cells with various patterned electrodes (*e.g.*, Ti, Au, Pt, etc.) and the simple design of two electrode configurations was used. In this type of liquid cell, liquid electrolyte is confined into a thin film between two SiN_x membranes. By controlling the thickness of the liquid layer and the membranes, improved resolution for *in situ* TEM imaging has been achieved. To avoid electrolyte depletion during the *in situ* TEM experiments,[1] we designed the electrical pads with wire bonding through the reservoirs, thus only limited areas of the electrode surfaces are exposed to the electrolyte (Figure 2f and **9 a**).[16] Using such Si/SiN_x electrochemical liquid cells, we studied the dendritic growth of Pb and Li, electrodeposition of other metals, such as Na and Mg, solid-electrolyte interphase (SEI) formation, and other phenomena with lithium batteries[17–18,84] or other[87] battery chemistry.

As the initial test experiments, electrodeposition and dissolution of Pb were achieved (Figure 9b).[16] By combining with detailed *ex situ* characterization of the Pb dendrites at different stages, crystallization pathways of Pb dendrites were unveiled. However, it was challenging to directly observe the growth of Li dendrites due to the poor imaging contrast, air sensitivity during sample preparation, etc. Figure 9c–d show the first direct observation of Li dendritic growth and SEI formation.[17–18] Further EDS mapping and four-dimensional scanning TEM (4D-STEM, then called nano-diffraction) analysis revealed the structure and chemistry of SEI. The Li dendrite growth[17] and lithiation of Si nanowires[89] are the

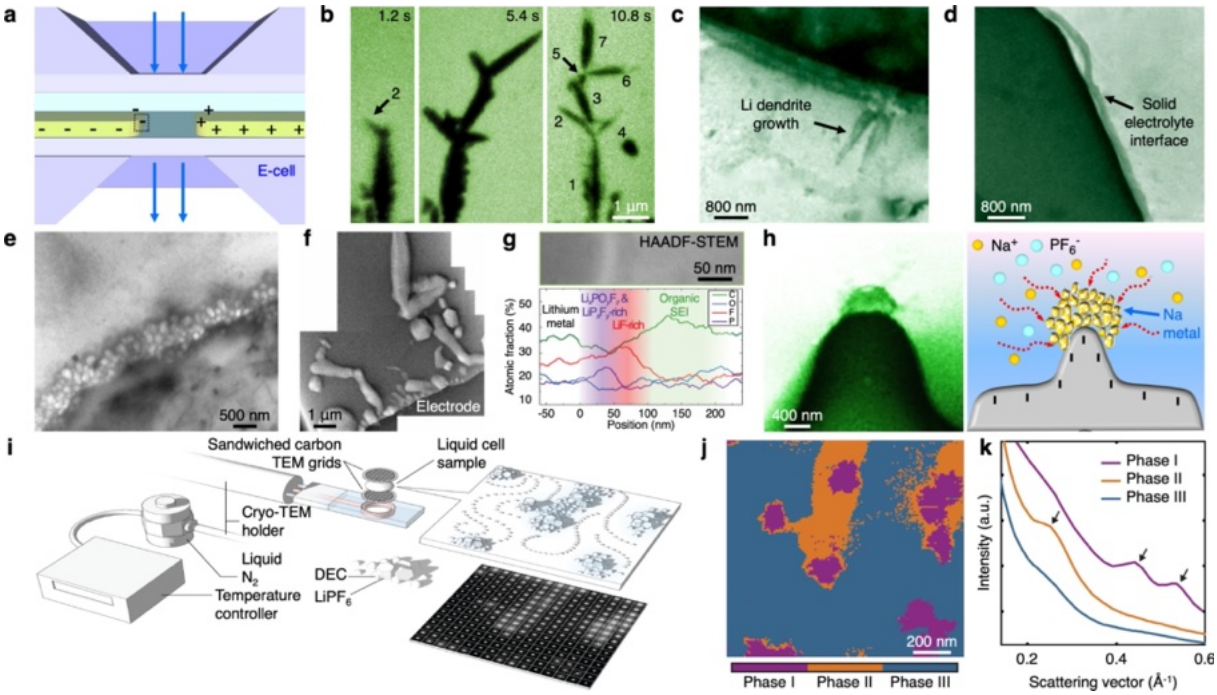

Figure 9. Liquid cell TEM studies of various physicochemical phenomena related to lithium batteries and beyond. (a) Schematic of a custom-made SiN_x electrochemical liquid cell (E-cell). Reproduced with permission. Copyright 2020, Elsevier Ltd.[88] (b) Sequential TEM images showing the growth and dissolution of Pb dendrites in the electrochemical liquid cell. Reproduced with permission. Copyright 2013, The Authors, under a Creative Commons Attribution-NonCommercial-ShareAlike 3.0 Unported License.[16] (c-d) TEM images displaying Li dendrite growth (c) and SEI formation (d) within the electrochemical liquid cell. Reproduced with permission. Copyright 2014, American Chemical Society, under an ACS AuthorChoice License.[17] (e) TEM image of Li metal nanogranular growth facilitated by a PDDA cationic polymer film coating on the electrodes of the electrochemical liquid cell. Reproduced with permission. Copyright 2020, The Royal Society of Chemistry.[84] (f) TEM image showing Li dendritic growth on electrodes without the PDDA polymer coating. Reproduced with permission. Copyright 2022, Elsevier Ltd.[86] (g) EDS elemental mapping and corresponding line profiles demonstrating a LiF-rich SEI layer. Reproduced with permission. Copyright 2020, The Royal Society of Chemistry.[84] (h) TEM image and corresponding schematic of electrochemical Na metal deposition on electrodes with sharp curvature in the liquid cell. Reproduced with permission. Copyright 2020, Elsevier Ltd.[88] (i) Illustration of the integrated approach using liquid cell TEM, modified Cryo-TEM, and 4D-STEM for studying highly beam-sensitive liquid organic electrolyte (1 M $LiPF_6$ in 1:1 EC:DEC) at cryogenic temperatures. (j-k) Deep-learning-based analysis of acquired 4D-STEM datasets enabling reconstruction of phase mapping (j) based on three classified phases (k). (i-k) Reproduced with permission. Copyright 2023, The Authors, under a Creative Commons Attribution-NonCommercial License 4.0.[93]

early success of electrochemical liquid cell TEM studies of lithium-ion batteries.

We extended our *in situ* studies of lithium deposition with increased complexity. By using a poly(diallyldimethylammonium chloride) (PDDA) polymer film to coat the electrodes in a liquid cell, we obtained nanogranular growth of lithium metal, which appeared to be drastically different from the dendritic growth of lithium on the bare electrodes (Figure 9e–f).[84] EDS chemical analysis showed a LiF-rich SEI layer (Figure 9g), which was responsible for the suppression of Li dendrites.[90] The nanoscale modifications of SEI structure and chemistry were due to $[PF_6]^-$ ions being accumulated at the electrode-electrolyte interfaces by the coating of cationic PDDA polymer film. It was remarkable that the LiF-rich SEI layer was achieved without increasing the electrolyte salt concentration.

We further studied the electrodeposition of Na metal on electrodes with varied surface roughness, in which a liquid electrolyte of 1 M $NaPF_6$ dissolved in propylene carbonate (PC) was used.[88] As shown in Figure 9h, the nucleation of Na only occurred on the nude of rough electrode surfaces, which was distinctly different from the uniform nucleation of Na on a flat electrode. This work is not only relevant to Na metal batteries but also provides insights into the impact of surface roughness of current collectors for the metal anode in general. Other studies of alternative batteries include the direct observation of uniform electrodeposition of Mg film. *In situ* scanning transmission X-ray microscopy (STXM) and X-ray absorption spectroscopy (XAS) identified the Mg thin film as hexa-coordinated organometallic Mg compounds, which are attributed to the observed non-reversibility.[87]

In addition, we studied the phase segregation and structural ordering of liquid electrolytes for lithium batteries (1 M $LiPF_6$ dissolved in 1 : 1 (v/v) ethylene carbonate (EC):diethylcarbonate (DEC)) at the low temperature by liquid-phase TEM integrated with cryogenic transmission electron microscopy (Cryo-TEM) operated at −30 °C, 4D-STEM, high energy resolution electron energy loss spectroscopy (EELS), and data analysis based on deep learning (Figure 9i–k).[93] We discovered the presence of short-range ordering (SRO) in the high salt-concentration domains of the low-temperature liquid electrolyte. MD simulations suggest the SRO originates from the Li^+-$(PF_6^-)_n$ ($n > 2$) local structural order induced by high $LiPF_6$ salt concentration.

Electrified Solid-Liquid Interfaces in Electrocatalysis

We developed polymer electrochemical liquid cells for *in situ* TEM study of electrified solid-liquid interfaces during electrocatalytic reactions.[29] High-resolution imaging of electrocatalyst surface restructuring at the atomic level was achieved (Figure 10a–c). Such polymer liquid cells also allow fast freezing of the liquid sample at certain states of reactions, which enables chemical analysis using EELS that is often hard to achieve in the liquid cell with fast-evolving dynamics during reactions. This innovative electrochemical liquid cell design opens new opportunities for *in situ* TEM study of various electrocatalytic reactions and many other electrochemical processes.

Using this setup, we studied Cu-catalyzed CO_2 reduction reaction (CO_2RR) focusing on the atomic dynamics of electrified solid-liquid interfaces. We found a fluctuating liquid-like amorphous interphase, which mediates the crystalline Cu surface restructuring and mass loss during CO_2RR.[29] In electrocatalysis, the interfaces between the catalyst and electrolyte are where the catalytic reactions occur, so the presence of intermediates and restructuring strongly impact the catalytic performance. Our revealing of the atomic dynamics of fluctuating liquid-like amorphous interphase has important implications, for example, using transient interphases to tune catalyst surface restructuring and thus the catalytic performance.

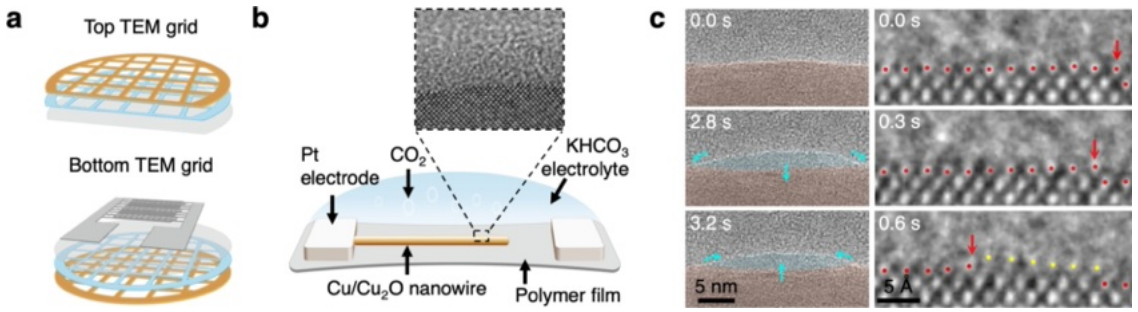

Figure 10. Development of a homemade polymer electrochemical liquid cell TEM revealing structural dynamics of Cu-based catalysts during electrochemical CO_2 reduction. (a) Illustration of the components of the new polymer liquid cell. (b) Schematic of a perspective view of the sample area inside the polymer electrochemical liquid cell, with an inset HRTEM image of the electrified solid-liquid interface. (c) Series of HRTEM images showing the fluid-like motion and transformation of the amorphous interphase (blue) between the solid catalyst (brown) and liquid electrolyte (gray) during electrochemical CO_2 reduction (left column) and revealing atomic-level changes in the Cu structure at the electrified solid-liquid interface (right column). (a-c) Reproduced with permission. Copyright 2024, The Authors, under exclusive license to Springer Nature Limited.[29]

In the future, using *operando* multimodal characterization, *e.g.*, high-resolution electrochemical liquid cell TEM and time-resolved XAS, it opens many opportunities for tracking the electrocatalyst morphological changes, structural and bonding evolution during CO_2RR or other electrocatalytic reactions (Figure 9d).

Data Analysis with Computer Vision and Machine Learning

The modern *in situ* TEM experiment with fast electron detection often generates large datasets. Computer-aided data analysis has become indispensable. The highlighted approaches from my group evolved from the computer-assisted tracking of nanoparticle movements[37] to nanoparticle 3D atomic structure of a nanoparticle by computer vision,[35] and revolving structural ordering in liquid electrolytes with machine learning.[93]

Understanding the structural order of materials is central to controlling their properties. The structural order of liquid electrolytes can impact a series of macroscopic parameters, such as ion ionic conductivity, ionic transport mode, and viscosity. However, determining the degree and the spatial extent of structural order in liquids is often a significant challenge. Through the collaborative effort,[93] we showed that machine-learning data analysis enabled the identification of short-range ordering in the low-temperature battery liquid electrolyte. The machine learning approach is expected to play an increasingly important role in liquid phase TEM experiments, or *in situ* TEM, in general.

Liquid Phase TEM Technology and Manufacturing

The development of high spatial resolution liquid phaseTEM has enabled breakthroughs in characterizing various chemical processes by allowing to unveil of materials transformation pathways, structure and bonding of liquid samples, dynamic phenomena at electrified solid-liquid interfaces related to batteries and electrocatalysis, and so on.[94] Compared with other *in situ* characterization methods, liquid phase TEM provides unique advantages. For example, *in situ* X-ray spectroscopy measurements provide ensemble information, but lack spatially resolved individual particle details.[98] Scanning probe microscopy can only present the surface properties of materials.[99] Optical microscopy has limited spatial resolution and thus cannot resolve structural and chemical transformations at the atomic or nanometer level, with the exception when chemical tags being used in specific applications.[100]

Liquid phase TEM technology has been widely used nowadays. There are half of a dozen companies providing commercial products, which include sample holders, liquid cells, and other accessories for liquid phase electron microscopy. Many research groups have developed their own liquid cells and sample holders. Our early research and development contributed to the commercial development of liquid sample holders and SiN_x liquid cell fabrication. Recently, our design of polymer electrochemical liquid cells and the corresponding sample holder design opened new opportunities for technology transfer into commercial products. Some key points on the fabrication of liquid cells and sample holders are highlighted as follows.

The liquid cells can be either self-contained or designed as a flow cell allowing liquids to flow in and out of the cell through nanotubing. The self-contained liquid cell design can adopt a variety of membranes, such as SiN_x,[8–9, 19, 95, 102] polymer membrane,[29] graphene,[20] amorphous carbon,[26] MoS_2,[27] BN,[28] or other 2D materials. So far, the commercial flow cells only use SiN_x as a membrane since it is more robust in handling.[102–103] It is also noted that since liquid flow generates liquid motion that may introduce image blurring, images/movies are often taken in a stationary liquid in most experiments using a flow cell.

The challenges of obtaining high resolution from liquid cell TEM experiments often arise from the fact that the liquid cell samples are too thick. By stacking or gluing two chips together, it was not able to reach the sub-nanometer image solution. Making thin freestanding membranes and controlling the liquid thickness are the key. However, for large scale fabrication of Si/SiN_x liquid cells, the thin wafers can be too fragile using standard Si wafers processes. By bonding the thin Si wafer (*e.g.*, 100 μm) to a standard Si (*e.g.*, 500 μm) using photoresist, it can address the issue (Figure 11a–b).

In situ TEM studies driven by electrochemical stimuli require a specialized experimental setup, including a TEM sample holder with electric biasing capabilities, a potentiostat for electrical input, and the sample cell. Thin electrochemical liquid cells were achieved by incorporating patterned electrodes onto the membrane of a chip. Our recently developed polymer electrochemical liquid cells (PLC) allow atomic-level imaging of electrified solid-liquid interfaces.[29] Such PLCs have large viewing windows and can accommodate fast freezing of the liquid cell without the membrane being shattered, which allows careful examination of certain reaction states using EELS, 4D-STEM, or other advanced microscopy techniques. Large-scale fabrication of such a new generation of electrochemical liquid cells and the corresponding sample holder will facilitate the research development (Figure 11c–e).

Conclusion and Outlook

In conclusion, by developing and applying liquid phase electron microscopy with high-resolution imaging at the atomic level and the ability to handle complex systems and reactions, it has opened unprecedented opportunities to study nanoscale materials transformations in liquid phase reactions and dynamic phenomena at solid-liquid interfaces. This article describes my personal journey in nanoscience and nanotechnology, highlighting my initial work and the efforts of my

Israel Journal of Chemistry

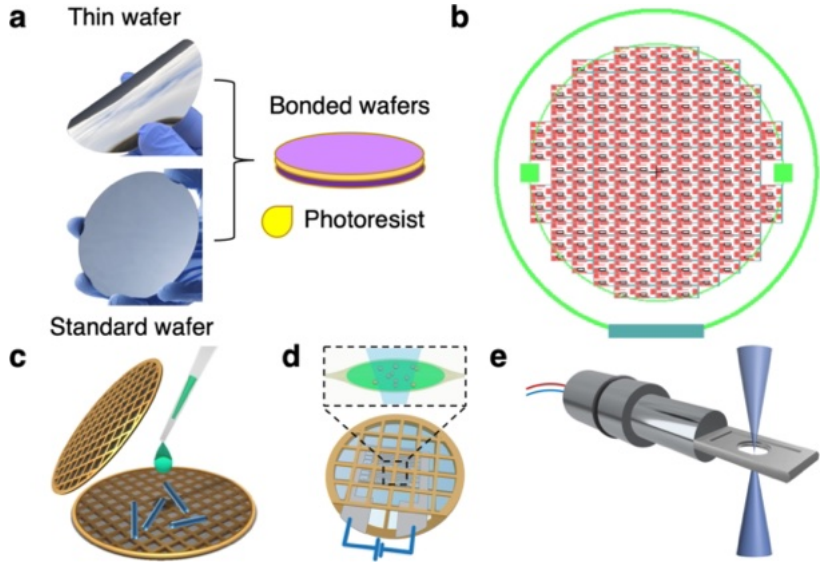

Figure 11. Development and fabrication of liquid cells and sample holder for enhanced liquid phase TEM technology. (a) A thin silicon wafer, 100 μm thick, was bonded to a standard silicon wafer, 500 μm thick, enabling automated lithographic patterning. (b) A photolithography mask was used for the batch fabrication of the SiN_x liquid cells. (a-b) Reproduced with permission. Copyright 2021, This is a U.S. government work and not under copyright protection in the U.S.; foreign copyright protection may apply, under a Creative Commons Attribution 4.0 International License.[94] (c) Schematic illustration of the preparation of a custom carbon film liquid cell. (d) Illustration of a homemade polymer electrochemical liquid cell. (c-d) Reproduced with permissions. Copyrights 2022, The Authors, under a Creative Commons Attribution 4.0 International License,[22] 2024, The Authors, under exclusive license to Springer Nature Limited.[29] (e) Schematic illustration of the development of TEM holders and sample stages tailored for investigating specific physicochemical phenomena using liquid cell TEM.

research group on developing and applying liquid phase electron microscopy for studying nucleation, growth and self-assembly of nanocrystals, solid-liquid interfaces, electrochemical processes in batteries, electrocatalysis, and others nanoscale dynamic phenomena. Insights garnered from this research enable novel materials synthesis, and efficient applications of materials in electrocatalysis, batteries and other functional devices. As a recent example, inspired by liquid cell TEM studies, we innovated materials synthesis by liquid interface engineering and achieved breakthroughs in synthesis of high entropy alloy nanomaterials.[104]

Liquid phase TEM as a powerful platform will continue to contribute uniquely to the future scientific explorations. My perspectives on the challenges and future opportunities are outlined as follows.

There are still limitations of the current liquid phase TEM platform. For example, the self-contained thin liquid cells are excellent for high-resolution imaging, but they only have a small amount of liquids and it is hard to control the reactions using a pre-mixed solution. For the flow cell design, since the motion of a flowing liquid may introduce image blurring, movies are often taken with a stationary liquid in the liquid cell. In addition, the liquid is often too thick for achieving atomic-resolution imaging. Future *development of liquid cells* to continue expand the liquid phase TEM capabilities is needed.

The *electron beam interactions* with the samples may introduce structural or chemical changes altering the intrinsic properties of materials. In general, controlling the electron dose rate and total dosage is essential for liquid phase TEM experiments. From another point, it opens opportunities to utilize the electron beam interactions with liquids, *e.g.*, electron beam induced radiolysis of water generates hydrogen and oxygen gases, which are useful for certain research topics. For example, liquid phase TEM has been utilized to study dynamic hydrogen intercalation into host materials.

Many liquid phase TEM experiments are conducted at room temperature. Reactions at elevated temperature as well as low (sub-zero) temperature have also been reporte by using different sample stages. The ability to vary the reaction temperatures of the same liquid sample in a wide temperature range will add an additional freedom in studying the reaction kinetics.

The *integrated advanced microscopy and spectroscopy techniques*, such as atomic resolution imaging, chemical analysis using EDS or EELS, structural analysis using electron diffraction, in-situ liquid cell TEM studies combing with Cryo-EM experiments and image analysis methods, multi-modal characterization of the same sample with different electron microscopy techniques and X-ray methods may further enrich the information that can be collected from the experiments.

Modern *in situ* TEM experiments with fast electron detection generate large dataset, which requires computer-aided data analysis. *Data analysis using machine learning*

approaches c play a more and more important role in the future.

The *high-resolution electrochemical liquid cell TEM* has opened many new opportunities to address challenging problems in electrocatalysis and nanoscale electrochemistry. Advancements in nanoscale electrochemical cells, including the precise control of electrical potential and characterization of reactants and reaction products will accelerate the scientific discoveries and the growth of the research field.

Lastly, due to the complexity of the liquid cell TEM experiments, various approaches and strategies have been applied. The multidisciplinary research has drawn researchers from diverse fields, including materials science, chemistry, physics, biology, as well as electron microscopy to explore the most exciting and challenging scientific questions. It has opened many opportunities by merging different expertise and approaches together, and it will continue to stimulate innovations and foster novel scientific discoveries.

Acknowledgments

This work was supported by the U.S. Department of Energy, Office of Science, Office of Basic Energy Sciences (BES), Materials Sciences and Engineering Division under Award Number DE-AC02-05-CH11231 within the in situ TEM program (KC22ZH). Work at the Molecular Foundry of Lawrence Berkeley National Laboratory (LBNL) was supported by the U.S. Department of Energy under Contract No. DE-AC02-05CH11231. I would like to thank my Ph.D. graduate student, Daewon Lee, for his help in preparing high resolution figures, references, and copyrights; also thank my postdoc Qiubo Zhang for his proofreading of this article.

References

[1] H. Zheng, J. Wang, S. E. Lofland, Z. Ma, L. Mohaddes-Ardabili, T. Zhao, L. Salamanca-Riba, S. R. Shinde, S. B. Ogale, F. Bai, D. Viehland, Y. Jia, D. G. Schlom, M. Wuttig, A. Roytburd, R. Ramesh, *Science* **2004**, *303*, 661.
[2] H. Zheng, Q. Zhan, F. Zavaliche, M. Sherburne, F. Straub, M. P. Cruz, L.-Q. Chen, U. Dahmen, R. Ramesh, *Nano Lett.* **2006**, *6*, 1401.
[3] H. Zheng, F. Straub, Q. Zhan, P.-L. Yang, W.-K. Hsieh, F. Zavaliche, Y.-H. Chu, U. Dahmen, R. Ramesh, *Adv. Mater.* **2006**, *18*, 2747.
[4] H. Zheng, J. Kreisel, Y. H. Chu, R. Ramesh, L. Salamanca-Riba, *Appl. Phys. Lett.* **2007**, *90*, 113113.
[5] S. H. Oh, Y. Kauffmann, C. Scheu, W. D. Kaplan, M. Rühle, *Science* **2005**, *310*, 661.
[6] I. M. Abrams, J. W. McBain, *J. Appl. Phys.* **1944**, *15*, 607.
[7] I. A. Blech, E. S. Meieran, *Appl. Phys. Lett.* **1967**, *11*, 263.
[8] M. J. Williamson, R. M. Tromp, P. M. Vereecken, R. Hull, F. M. Ross, *Nat. Mater.* **2003**, *2*, 532.
[9] H. Zheng, R. K. Smith, Y.-w. Jun, C. Kisielowski, U. Dahmen, A. P. Alivisatos, *Science* **2009**, *324*, 1309.
[10] H. Zheng, S. A. Claridge, A. M. Minor, A. P. Alivisatos, U. Dahmen, *Nano Lett.* **2009**, *9*, 2460.
[11] H. L. Xin, H. Zheng, *Nano Lett.* **2012**, *12*, 1470.
[12] H.-G. Liao, L. Cui, S. Whitelam, H. Zheng, *Science* **2012**, *336*, 1011.
[13] H.-G. Liao, D. Zherebetskyy, H. Xin, C. Czarnik, P. Ercius, H. Elmlund, M. Pan, L.-W. Wang, H. Zheng, *Science* **2014**, *345*, 916.
[14] W.-I. Liang, X. Zhang, Y. Zan, M. Pan, C. Czarnik, K. Bustillo, J. Xu, Y.-H. Chu, H. Zheng, *J. Am. Chem. Soc.* **2015**, *137*, 14850.
[15] W.-I. Liang, X. Zhang, K. Bustillo, C.-H. Chiu, W.-W. Wu, J. Xu, Y.-H. Chu, H. Zheng, *Chem. Mater.* **2015**, *27*, 8146.
[16] M. Sun, H.-G. Liao, K. Niu, H. Zheng, *Sci. Rep.* **2013**, *3*, 3227.
[17] Z. Zeng, W.-I. Liang, H.-G. Liao, H. L. Xin, Y.-H. Chu, H. Zheng, *Nano Lett.* **2014**, *14*, 1745.
[18] Z. Zeng, X. Zhang, K. Bustillo, K. Niu, C. Gammer, J. Xu, H. Zheng, *Nano Lett.* **2015**, *15*, 5214.
[19] W. Zheng, D. Lee, H. Zheng, *MRS Bull.* **2024**, *49*, 205.
[20] J. M. Yuk, J. Park, P. Ercius, K. Kim, D. J. Hellebusch, M. F. Crommie, J. Y. Lee, A. Zettl, A. P. Alivisatos, *Science* **2012**, *336*, 61.
[21] D. Li, M. H. Nielsen, J. R. I. Lee, C. Frandsen, J. F. Banfield, J. J. De Yoreo, *Science* **2012**, *336*, 1014.
[22] Q. Zhang, X. Peng, Y. Nie, Q. Zheng, J. Shangguan, C. Zhu, K. C. Bustillo, P. Ercius, L. Wang, D. T. Limmer, H. Zheng, *Nat. Commun.* **2022**, *13*, 2211.
[23] H. Cho, M. R. Jones, S. C. Nguyen, M. R. Hauwiller, A. Zettl, A. P. Alivisatos, *Nano Lett.* **2017**, *17*, 414.
[24] S. Keskin, N. de Jonge, *Nano Lett.* **2018**, *18*, 7435.
[25] L. A. Bultema, R. Bücker, E. C. Schulz, F. Tellkamp, J. Gonschior, R. J. D. Miller, G. H. Kassier, *Ultramicroscopy* **2022**, *240*, 113579.
[26] C. Zhu, S. Liang, E. Song, Y. Zhou, W. Wang, F. Shan, Y. Shi, C. Hao, K. Yin, T. Zhang, J. Liu, H. Zheng, L. Sun, *Nat. Commun.* **2018**, *9*, 421.
[27] J. Yang, M. K. Choi, Y. Sheng, J. Jung, K. Bustillo, T. Chen, S.-W. Lee, P. Ercius, J. H. Kim, J. H. Warner, E. M. Chan, H. Zheng, *Nano Lett.* **2019**, *19*, 1788.
[28] J. R. Jokisaari, J. A. Hachtel, X. Hu, A. Mukherjee, C. Wang, A. Konecna, T. C. Lovejoy, N. Dellby, J. Aizpurua, O. L. Krivanek, J.-C. Idrobo, R. F. Klie, *Adv. Mater.* **2018**, *30*, 1802702.
[29] Q. Zhang, Z. Song, X. Sun, Y. Liu, J. Wan, S. B. Betzler, Q. Zheng, J. Shangguan, K. C. Bustillo, P. Ercius, P. Narang, Y. Huang, H. Zheng, *Nature* **2024**, *630*, 643.
[30] R. F. Egerton, P. Li, M. Malac, *Micron* **2004**, *35*, 399.
[31] T. J. Woehl, T. Moser, J. E. Evans, F. M. Ross, *MRS Bull.* **2020**, *45*, 746.
[32] M. Wang, C. Park, T. J. Woehl, *Chem. Mater.* **2018**, *30*, 7727.
[33] J. Korpanty, L. R. Parent, N. C. Gianneschi, *Nano Lett.* **2021**, *21*, 1141.
[34] I. A. Moreno-Hernandez, M. F. Crook, J. C. Ondry, A. P. Alivisatos, *J. Am. Chem. Soc.* **2021**, *143*, 12082.
[35] Y. Wang, X. Peng, A. Abelson, P. Xiao, C. Qian, L. Yu, C. Ophus, P. Ercius, L.-W. Wang, M. Law, H. Zheng, *Sci. Adv.* **2019**, *5*, eaaw5623.
[36] J. Yang, Z. Zeng, J. Kang, S. Betzler, C. Czarnik, X. Zhang, C. Ophus, C. Yu, K. Bustillo, M. Pan, J. Qiu, L.-W. Wang, H. Zheng, *Nat. Mater.* **2019**, *18*, 970.
[37] A. S. Powers, H.-G. Liao, S. N. Raja, N. D. Bronstein, A. P. Alivisatos, H. Zheng, *Nano Lett.* **2017**, *17*, 15.
[38] Y. Wang, X. Peng, A. Abelson, B.-K. Zhang, C. Qian, P. Ercius, L.-W. Wang, M. Law, H. Zheng, *Nano Res.* **2019**, *12*, 2549.

[39] N. C. Anderson, M. P. Hendricks, J. J. Choi, J. S. Owen, *J. Am. Chem. Soc.* **2013**, *135*, 18536.
[40] J. W. Gibbs, *The Collected Works of J. Willard Gibbs, Vol. 1: Thermodynamics* (Eds.: H. A. Bumstead, R. G. Van Name, W. R. Longley), Longmans, Green and Company, New York, London, Toronto, **1928**.
[41] G. Wulff, *Z. Kristallogr. Mineral.* **1901**, *34*, 449.
[42] Y. Xia, Y. Xiong, B. Lim, S. E. Skrabalak, *Angew. Chem. Int. Ed.* **2009**, *48*, 60.
[43] N. Tian, Z.-Y. Zhou, S.-G. Sun, Y. Ding, Z. L. Wang, *Science* **2007**, *316*, 732.
[44] C. R. Bealing, W. J. Baumgardner, J. J. Choi, T. Hanrath, R. G. Hennig, *ACS Nano* **2012**, *6*, 2118.
[45] E. Ringe, R. P. Van Duyne, L. D. Marks, *Nano Lett.* **2011**, *11*, 3399.
[46] C. Schliehe, B. H. Juarez, M. Pelletier, S. Jander, D. Greshnykh, M. Nagel, A. Meyer, S. Foerster, A. Kornowski, C. Klinke, H. Weller, *Science* **2010**, *329*, 550.
[47] S. Gao, Y. Sun, F. Lei, L. Liang, J. Liu, W. Bi, B. Pan, Y. Xie, *Angew. Chem. Int. Ed.* **2014**, *53*, 12789.
[48] J. S. Son, X.-D. Wen, J. Joo, J. Chae, S.-i. Baek, K. Park, J. H. Kim, K. An, J. H. Yu, S. G. Kwon, S.-H. Choi, Z. Wang, Y.-W. Kim, Y. Kuk, R. Hoffmann, T. Hyeon, *Angew. Chem. Int. Ed.* **2009**, *48*, 6861.
[49] S. Sun, H. Zeng, D. B. Robinson, S. Raoux, P. M. Rice, S. X. Wang, G. Li, *J. Am. Chem. Soc.* **2004**, *126*, 273.
[50] J. S. Son, J. H. Yu, S. G. Kwon, J. Lee, J. Joo, T. Hyeon, *Adv. Mater.* **2011**, *23*, 3214.
[51] W. Z. Ostwald, *Z. Phys. Chem.* **1901**, *37*, 385.
[52] P. Sahu, B. L. V. Prasad, *Nanoscale* **2013**, *5*, 1768.
[53] Z. A. Peng, X. Peng, *J. Am. Chem. Soc.* **2001**, *123*, 1389.
[54] C. K. Narula, X. Yang, C. Li, A. R. Lupini, S. J. Pennycook, *J. Phys. Chem. C* **2015**, *119*, 25114.
[55] Q. Zheng, J. Shangguan, X. Li, Q. Zhang, K. C. Bustillo, L.-W. Wang, J. Jiang, H. Zheng, *Nano Lett.* **2021**, *21*, 6640.
[56] X. Peng, J. Shangguan, Q. Zhang, M. Hauwiller, H. Yu, Y. Nie, K. C. Bustillo, A. P. Alivisatos, M. Asta, H. Zheng, *Nano Lett.* **2024**, *24*, 1168.
[57] A. Moosavi, M. Rauscher, S. Dietrich, *Phys. Rev. Lett.* **2006**, *97*, 236101.
[58] U. M. Mirsaidov, H. Zheng, D. Bhattacharya, Y. Casana, P. Matsudaira, *Proc. Natl. Acad. Sci. USA* **2012**, *109*, 7187.
[59] A. Chakrabarti, G. P. T. Choi, L. Mahadevan, *Phys. Rev. Lett.* **2020**, *124*, 258002.
[60] M. Moseler, U. Landman, *Science* **2000**, *289*, 1165.
[61] B. Barker, J. B. Bell, A. L. Garcia, *Proc. Natl. Acad. Sci. USA* **2023**, *120*, e2306088120.
[62] H.-G. Liao, H. Zheng, *J. Am. Chem. Soc.* **2013**, *135*, 5038.
[63] S. Chandrasekhar, *Hydrodynamic and hydromagnetic stability*, Dover Publications, Inc., New York, **1981**.
[64] F. Kassubek, C. A. Stafford, G. Hermann, E. G. Raymond, *Nonlinearity* **2001**, *14*, 167.
[65] S. Jeon, T. Heo, S.-Y. Hwang, J. Ciston, K. C. Bustillo, B. W. Reed, J. Ham, S. Kang, S. Kim, J. Lim, K. Lim, J. S. Kim, M.-H. Kang, R. S. Bloom, S. Hong, K. Kim, A. Zettl, W. Y. Kim, P. Ercius, J. Park, W. C. Lee, *Science* **2021**, *371*, 498.
[66] X. Zhang, S. Han, B. Zhu, G. Zhang, X. Li, Y. Gao, Z. Wu, B. Yang, Y. Liu, W. Baaziz, O. Ersen, M. Gu, J. T. Miller, W. Liu, *Nat. Catal.* **2020**, *3*, 411.
[67] G. Prieto, J. Zečević, H. Friedrich, K. P. de Jong, P. E. de Jongh, *Nat. Mater.* **2013**, *12*, 34.
[68] M. Capdevila-Cortada, *Nat. Catal.* **2020**, *3*, 860.
[69] R. Ouyang, J.-X. Liu, W.-X. Li, *J. Am. Chem. Soc.* **2013**, *135*, 1760.
[70] Y. Liu, Y. Yang, Y. Sun, J. Song, N. G. Rudawski, X. Chen, W. Tan, *J. Am. Chem. Soc.* **2019**, *141*, 7407.
[71] H. Ma, S. Kang, S. Lee, G. Park, Y. Bae, G. Park, J. Kim, S. Li, H. Baek, H. Kim, J.-S. Yu, H. Lee, J. Park, J. Yang, *ACS Nano* **2023**, *17*, 13734.
[72] X. Peng, A. Abelson, Y. Wang, C. Qian, J. Shangguan, Q. Zhang, L. Yu, Z.-W. Yin, W. Zheng, K. C. Bustillo, X. Guo, H.-G. Liao, S.-G. Sun, M. Law, H. Zheng, *Chem. Mater.* **2019**, *31*, 190.
[73] W. Zheng, J. Kang, K. Niu, C. Ophus, E. M. Chan, P. Ercius, L.-W. Wang, J. Wu, H. Zheng, *Sci. Adv.* **2024**, *10*, eadn6426.
[74] K. Niu, T. Frolov, H. L. Xin, J. Wang, M. Asta, H. Zheng, *Proc. Natl. Acad. Sci. USA* **2015**, *112*, 12928.
[75] X. Peng, F.-C. Zhu, Y.-H. Jiang, J.-J. Sun, L.-P. Xiao, S. Zhou, K. C. Bustillo, L.-H. Lin, J. Cheng, J.-F. Li, H.-G. Liao, S.-G. Sun, H. Zheng, *Nat. Commun.* **2022**, *13*, 3601.
[76] J. Li, Y. Zhu, W. Chen, Z. Lu, J. Xu, A. Pei, Y. Peng, X. Zheng, Z. Zhang, S. Chu, Y. Cui, *Joule* **2019**, *3*, 557.
[77] Z. Liu, X. Sheng, D. Wang, X. Feng, *iScience* **2019**, *17*, 67.
[78] W. Wang, T. Xu, J. Chen, J. Shangguan, H. Dong, H. Ma, Q. Zhang, J. Yang, T. Bai, Z. Guo, H. Fang, H. Zheng, L. Sun, *Nat. Mater.* **2022**, *21*, 859.
[79] C. Choi, S. Kwon, T. Cheng, M. Xu, P. Tieu, C. Lee, J. Cai, H. M. Lee, X. Pan, X. Duan, W. A. Goddard, Y. Huang, *Nat. Catal.* **2020**, *3*, 804.
[80] J. T. Mefford, A. R. Akbashev, M. Kang, C. L. Bentley, W. E. Gent, H. D. Deng, D. H. Alsem, Y.-S. Yu, N. J. Salmon, D. A. Shapiro, P. R. Unwin, W. C. Chueh, *Nature* **2021**, *593*, 67.
[81] M. Liu, Y. Pang, B. Zhang, P. De Luna, O. Voznyy, J. Xu, X. Zheng, C. T. Dinh, F. Fan, C. Cao, F. P. G. de Arquer, T. S. Safaei, A. Mepham, A. Klinkova, E. Kumacheva, T. Filleter, D. Sinton, S. O. Kelley, E. H. Sargent, *Nature* **2016**, *537*, 382.
[82] M. J. Zachman, Z. Tu, S. Choudhury, L. A. Archer, L. F. Kourkoutis, *Nature* **2018**, *560*, 345.
[83] A. Molinari, P. M. Leufke, C. Reitz, S. Dasgupta, R. Witte, R. Kruk, H. Hahn, *Nat. Commun.* **2017**, *8*, 15339.
[84] S.-Y. Lee, J. Shangguan, J. Alvarado, S. Betzler, S. J. Harris, M. M. Doeff, H. Zheng, *Energy Environ. Sci.* **2020**, *13*, 1832.
[85] Z. Zeng, W.-I. Liang, Y.-H. Chu, H. Zheng, *Faraday Discuss.* **2014**, *176*, 95.
[86] S.-Y. Lee, J. Shangguan, S. Betzler, S. J. Harris, M. M. Doeff, H. Zheng, *Nano Energy* **2022**, *102*, 107641.
[87] Y. A. Wu, Z. Yin, M. Farmand, Y.-S. Yu, D. A. Shapiro, H.-G. Liao, W.-I. Liang, Y.-H. Chu, H. Zheng, *Sci. Rep.* **2017**, *7*, 42527.
[88] Z. Zeng, P. Barai, S.-Y. Lee, J. Yang, X. Zhang, W. Zheng, Y.-S. Liu, K. C. Bustillo, P. Ercius, J. Guo, Y. Cui, V. Srinivasan, H. Zheng, *Nano Energy* **2020**, *72*, 104721.
[89] M. Gu, L. R. Parent, B. L. Mehdi, R. R. Unocic, M. T. McDowell, R. L. Sacci, W. Xu, J. G. Connell, P. Xu, P. Abellan, X. Chen, Y. Zhang, D. E. Perea, J. E. Evans, L. J. Lauhon, J.-G. Zhang, J. Liu, N. D. Browning, Y. Cui, I. Arslan, C.-M. Wang, *Nano Lett.* **2013**, *13*, 6106.
[90] Y. Gao, Z. Yan, J. L. Gray, X. He, D. Wang, T. Chen, Q. Huang, Y. C. Li, H. Wang, S. H. Kim, T. E. Mallouk, D. Wang, *Nat. Mater.* **2019**, *18*, 384.
[91] Y. Sun, Y. Zhao, J. Wang, J. Liang, C. Wang, Q. Sun, X. Lin, K. R. Adair, J. Luo, D. Wang, R. Li, M. Cai, T.-K. Sham, X. Sun, *Adv. Mater.* **2019**, *31*, 1806541.
[92] J. Luo, C.-C. Fang, N.-L. Wu, *Adv. Energy Mater.* **2018**, *8*, 1701482.
[93] Y. Xie, J. Wang, B. H. Savitzky, Z. Chen, Y. Wang, S. Betzler, K. Bustillo, K. Persson, Y. Cui, L.-W. Wang, C. Ophus, P. Ercius, H. Zheng, *Sci. Adv.* **2023**, *9*, eadc9721.

Israel Journal of Chemistry

[94] H. Zheng, *MRS Bull.* **2021**, *46*, 443.
[95] U. Mirsaidov, J. P. Patterson, H. Zheng, *MRS Bull.* **2020**, *45*, 704.
[96] P. Ercius, J. A. Hachtel, R. F. Klie, *MRS Bull.* **2020**, *45*, 761.
[97] Q. Zhang, D. Lee, H. Zheng, *Nano Res.* **2024**, *17*, 9152.
[98] L. Wu, J. J. Willis, I. S. McKay, B. T. Diroll, J. Qin, M. Cargnello, C. J. Tassone, *Nature* **2017**, *548*, 197.
[99] Q. Chen, J. M. Yuk, M. R. Hauwiller, J. Park, K. S. Dae, J. S. Kim, A. P. Alivisatos, *MRS Bull.* **2020**, *45*, 713.
[100] W. Xu, J. S. Kong, Y.-T. E. Yeh, P. Chen, *Nat. Mater.* **2008**, *7*, 992.
[101] P. Chen, X. Zhou, H. Shen, N. M. Andoy, E. Choudhary, K.-S. Han, G. Liu, W. Meng, *Chem. Soc. Rev.* **2010**, *39*, 4560.
[102] N. de Jonge, F. M. Ross, *Nat. Nanotechnol.* **2011**, *6*, 695.
[103] N. de Jonge, D. B. Peckys, G. J. Kremers, D. W. Piston, *Proc. Natl. Acad. Sci. USA* **2009**, *106*, 2159.
[104] H. Zheng, Q. Zhang, Y. Chen, Patent app. number 63/651,592 (2024).

Manuscript received: August 13, 2024
Version of record online: December 2, 2024